CHEMIJA. 2022. Vol. 33. No. 4. P. 127–135

Aqueous sol–gel synthesis, thermoanalytical, structural and vibrational studies of lithium aluminium molybdate ($LiAlMo_2O_8$)

Artūras Žalga[*], **Austėja Diktanaitė**, **Giedrė Gaidamavičienė**

Department of Applied Chemistry, Institute of Chemistry, Faculty of Chemistry and Geosciences, Vilnius University, 24 Naugarduko Street, 03225 Vilnius, Lithuania

Aqueous tartaric acid-assisted sol–gel preparation technique was successfully applied to synthesise lithium aluminium molybdate with the initial composition of $LiAl(MoO_4)_2$. From the results of the thermal analysis and X-ray diffraction measurement, the effect of tartaric acid as a ligand on the formation of homogeneous gel precursor was discussed. Besides, X-ray diffraction also revealed the crystallisation of the final $LiAlMo_2O_8$ ceramic below the temperature of 400°C. It was found that the initial composition of obtained ceramic significantly affected the formation of the impurity phase defined as $AlMo_2O_{12}$. The Rietveld refinement of the crystalline samples showed the tendency of crystallites growing with the increase of heat-treatment temperature. Similar trends of particle growing were also observed in the images of scanning electron microscopy (SEM) for the corresponding samples heat-treated at different temperatures. Finally, the Fourier-transform infrared spectroscopy (FT-IR) revealed the effect of both the surface morphology and the crystallite size on the intensity of characteristic vibration of the corresponding chemical bonds.

Keywords: sol–gel synthesis, thermal analysis, X-ray diffraction, Rietveld refinement, FT-IR spectroscopy

INTRODUCTION

$LiAl(MoO_4)_2$ belongs to the triclinic crystal system with the space group P-1. Its crystal structure is composed of LiO_5-trigonal bipyramid and AlO_6-octahedron layered, connected by isolated MoO_4-tetrahedron layered. In such cases, the MoO_4-tetrahedron and AlO_6-octahedron are connected by shared O atoms [1]. The modification of this multicomponent oxide system by transition metals and rare earth elements enhances its thermal stability and creates additional functions for use in different applications [2–6]. The most common and convenient preparation technique for such ceramic materials is related to the direct mixing of starting compounds [7], usually metal oxides, and the final heat treatment of the obtained mixture at relatively high temperatures. In this case, the complete homogenisation of the reaction mixture usually remains the most complicated part of this synthesis, and it takes lots of time and effort. Conversely, the solution-based methods [8–10], supported by the dissolution of organometallic compounds in nonaqueous media for better and easier mixing of the initial components at the molecular level, resulting in a better homogeneity and phase purity of the final ceramic compound, are rather complicated, expensive and have enhanced

[*] Corresponding author. Email: arturas.zalga@chf.vu.lt

toxicity. Thus, in this case, the synthesis way that enables the easy production of the homogeneous mixture of the starting compounds with enhanced safety and environmental friendliness is highly desirable. The possible solution to this problem may be directly related to the modification of the discussed synthesis techniques. Therefore, the elimination of the starting organometallic compounds from the synthesis procedure creates a novel solution-based synthesis approach, which expands the preparation possibilities for different multicomponent metal oxides and gives a strong additional novelty to this study. Furthermore, the introduction of aqueous media in the mixing stage of individual components at the molecular level [11] significantly decreases the cost of this process and increases its environmental friendliness [12–15]. In this work, we propose an aqueous tartaric acid-assisted sol-gel synthesis technique for the preparation of lithium aluminium molybdate for $LiAlMo_2O_8$ ceramic. Moreover, despite expected changes in surface morphology according to the increase of heat-treatment, the peculiarities of the crystalline phase formation also reveal the possible physical characteristics of the final crystalline mixture.

EXPERIMENTAL

The synthesis of Li–Al–Mo–O tartrate gel precursor for $LiAlMo_2O_8$ ceramic was prepared by an aqueous sol–gel synthesis by using tartaric acid as a chelating agent that interacts as a ligand at the molecular level with the reaction mixture during both dissolution in water and sol–gel formation. The general synthesis scheme of this experiment is illustrated and presented in Fig. 1, respectively.

In the first stage of this preparation technique, the powder of molybdenum (VI) oxide (MoO_3, 99.95%, Alfa Aesar) was dissolved in a small amount of the concentrated aqueous solution ($NH_3 \cdot H_2O$, 25% Penta). As shown in Equation 1 (Eq. 1), the molybdenum (VI) oxide dissolves in a hot concentrated ammonia solution forming NH_4^+ and MoO_4^{2-} ions.

$$MoO_3\,(s) + 2\,NH_3 \cdot H_2O\,(aq) \rightarrow$$

$$2\,NH_4^+\,(aq) + MoO_4^{2-}\,(aq) + 2\,H_2O\,(l). \qquad (1)$$

Excess ammonia is removed from the reaction mixture during further heating of the reaction mixture until 90% of the water is evaporated.

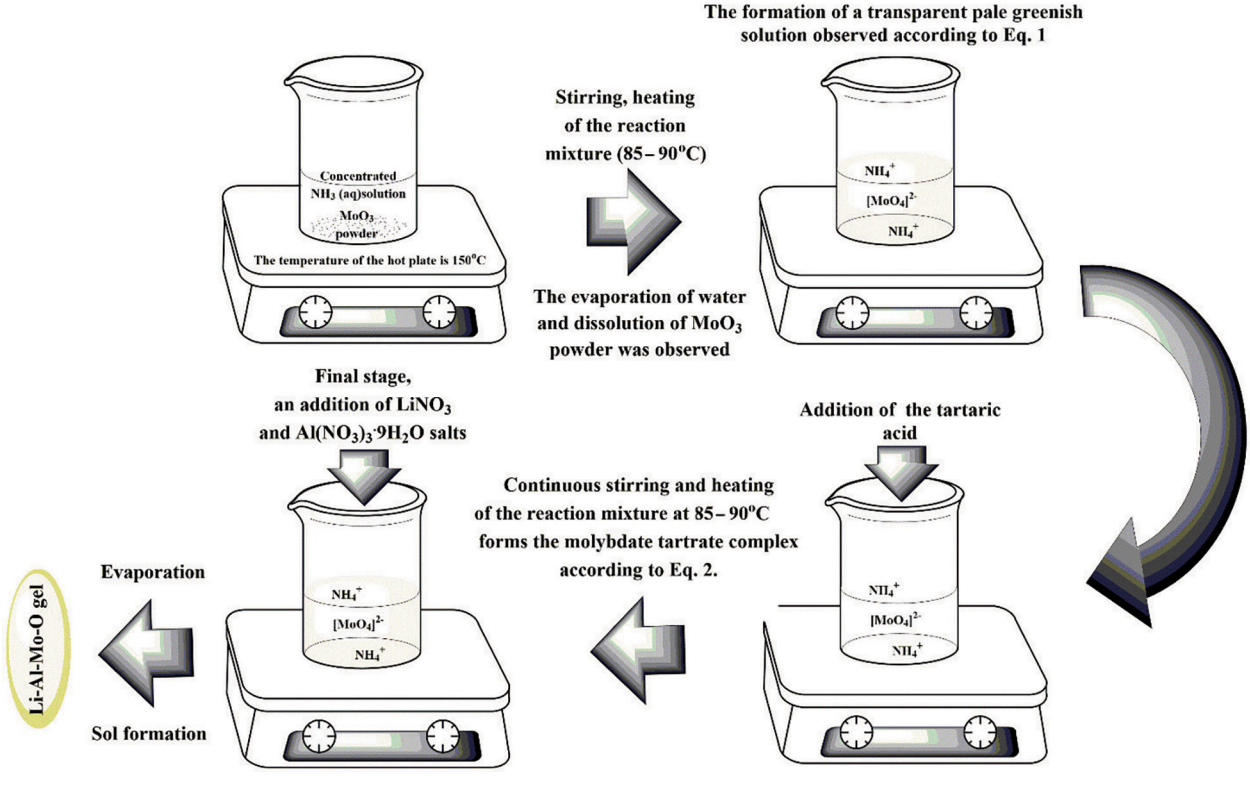

Fig. 1. Synthesis scheme of Li–Al–Mo–O tartrate precursor for $LiAlMo_2O_8$ ceramic

The addition of tartaric acid (L–(+)–tartaric acid ($C_4H_6O_6$) (TA) 99.5% Roth) to the reaction mixture creates a coordination compound for $[(MoO_4)_p(C_4H_4O_6)_qH_r]^{(2p+2q-r)-}$ composition [16, 17]. Generally, the chemical reaction that occurred after this procedure can be written as shown in Eq. 2:

$$P\ (NH_4)_2MoO_4\ (aq) + q\ C_4H_6O_6\ (aq) \rightarrow$$

$$[(MoO_4)_p(C_4H_4O_6)_qH_r]^{(2p+2q-r)-}\ (aq) +$$

$$2p\ NH_4^+\ (aq). \qquad (2)$$

Such a protective environment against pH changes is easily created by tartaric acid, which coordinates the corresponding molybdate complexes and prevents the occurring hydrolysis reaction that results in the formation of precipitates. Next to that followed the addition of lithium nitrate ($LiNO_3$, 99%, Alfa Aesar) and aluminium (III) nitrate nonahydrate ($Al(NO_3)_3{\cdot}9H_2O$, 99%, Alfa Aesar) into the reaction mixture, the obtained clear solution was additionally stirred in an open beaker at 85–90°C for several hours. Finally, a clear pale yellowish sol of corresponding metal ions was obtained and subsequently concentrated by slowly vapourising the reaction mixture at 90°C. After drying in an oven at 120°C, fine-grained light yellow gel powders were obtained. To show the crystal growth tendency, the well-milled Li–Al–Mo–O tartrate gel precursor was heat-treated at the temperatures of 400, 450, 500, 550, 600, 650 and 700°C.

The TG/DTA measurement of the Li–Al–Mo–O tartrate gel precursor was performed with a TG-DSC, STA 6000 Perkin-Elmer instrument using a sample weight of about 5 mg and a heating rate of 20 °/min under the continuous either air flow (20 cm^3/min) at ambient pressure from room temperature to 950°C. X-ray diffraction (XRD) patterns were recorded in air at room temperature by employing a powder X-ray diffractometer Rigaku MiniFlex II using Cu Kα radiation. XRD patterns were recorded at the standard rate of 1.5 2θ min^{-1}. The sample was spread on a glass holder to obtain the maximum intensity of the characteristic peaks in the XRD diffractograms. The Rietveld refinements of the obtained XRD patterns were performed using the X'Pert HighScore Plus software. A scanning electron microscope (SEM) Hitachi SU-70 was used to study the surface morphology and microstructure of the obtained ceramic samples. The characteristic vibrations of the functional groups in all heat-treated samples were estimated using a Perkin-Elmer Frontier FTIR spectrometer.

RESULTS AND DISCUSSION

Thermal analysis

In this work, the thermal analysis as a powerful tool was properly used for combustion of the as-prepared gel precursor, which plays an important role during the formation of the final ceramic. The decomposition process of the gel was performed in air atmosphere and the corresponding TG–DTG–DTA curves are shown in Fig. 2, respectively. In this case, the decomposition of the Li–Al–Mo–O tartrate gel precursor can be roughly divided into five main stages. The first mass change is directly related to an excess of tartaric acid, which has been added to the reaction mixture to avoid precipitation during the gelation process. This decomposition stage is well-seen from the TGA curve in the range of temperatures from 30 to 320°C. Although the synthesised gel was dried at 120°C temperature, the water molecules, which formed during the dimerisation of tartaric acid (Eq. 3), evaporated up to 125°C. Such removal of moisture from the gel powder could be confirmed by a broad endothermic band in the DTA curve.

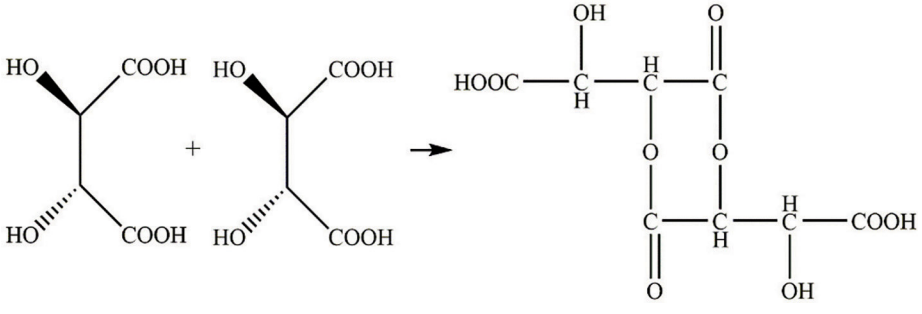

(3)

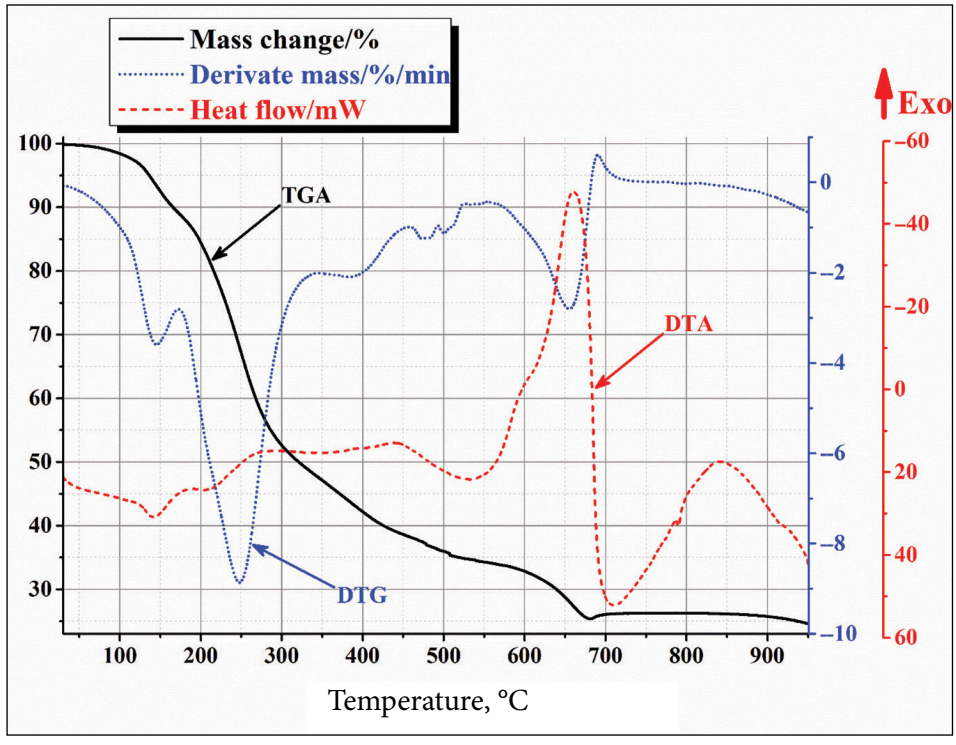

Fig. 2. Combined TG–DTG–DTA curves of the Li–Al–Mo–O tartrate gel precursor for $LiAlMo_2O_8$ ceramic by heat-treating in the air atmosphere

Further increase in the temperature leads to the evaporation of acetic acid that forms after the decomposition of the tartaric acid dimer. This process starts at about 130°C and ends at 175°C. It is also confirmed either by the well-expressed endothermic peak in the DTA curve or by the sharp band in the TGA curve. The exchange of hydrogen by hydroxyl group, known as Beckmann transformation, and the decomposition of an as-formed tartaric acid dimer are presented in Eq. 4, respectively:

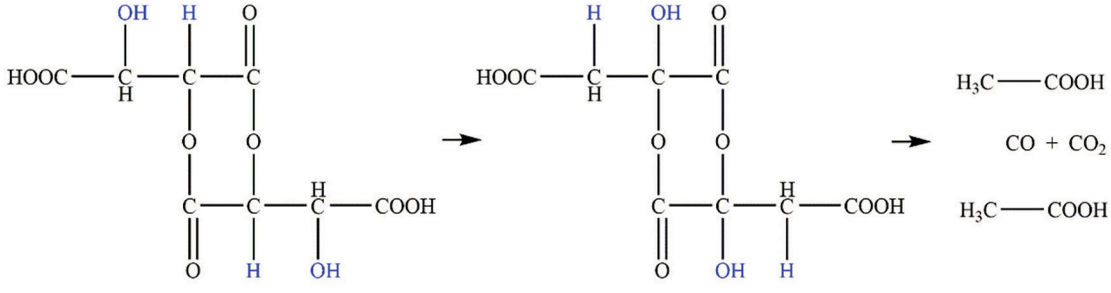

(4)

By further increasing the heating temperature, the formed tartaric acid dimer decomposes in a different manner. This process starts at 200°C and ends above 300°C. The release of carbon dioxide is confirmed by the broad exothermic band in the DTA curve. Meanwhile, the formation mechanism of pyruvic acid is shown in Eq. 5:

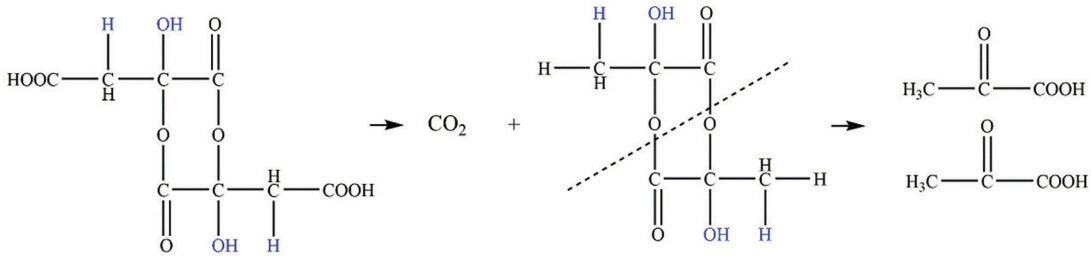

(5)

The total mass change in the temperature range of 30–320°C consists of about 50%, which is in good agreement with the amount of tartaric acid that was added to the reaction mixture at the beginning of the reaction. The further increase of the temperature from about 320 to 500°C is directly related to the thermal decomposition of the metal tartrates. This is partially confirmed by the small and broad exothermic bands in the DTA curve. It is also important to note that from the temperature of 450°C, an endothermic process is distinguished in the DTA curve, which is associated with the beginning of the crystallisation of multicomponent oxides. Next to that, in the range of temperature from 540 to 679°C, the occurring mass change (9.2%) is directly related to the combustion processes of inorganic carbon, which formed during the partial decomposition of metal tartrates at lower temperatures. The mass increase of the residue of the gel precursor in the range of temperature from 679 to 700°C is attributed to the formation of lithium peroxide, which absorbs the oxygen gas from lithium oxide as an impurity phase [18]. By further increasing the heating temperature above 730°C, the mass of the sample becomes stable. However, from 850°C, the mass change of the gel residue is observed, which is attributed to the decomposition of aluminium molybdate and the evaporation of molybdenum oxide.

Summarising the results of the thermal analysis, it is obvious that the formation of the obtained $LiAlMo_2O_8$ ceramic is highly dependent on the molar ratio of the initial reactants in the reaction mixture. The relatively low crystallisation temperature of $Al_2Mo_3O_{12}$ creates conditions for the formation of impurity compounds, the existence of which is evidenced by the increase in the mass of the residue of Li–Al–Mo–O tartrate gel precursor at the temperature of about 679°C. Moreover, the decrease in the mass of the sample powder above 850°C confirms the formation of aluminium molybdate in the crystalline mixture as an impurity phase.

X-ray diffraction

In this work, the XRD analysis of Li–Al–Mo–O tartrate gel precursor for the ceramic of the initial composition of $LiAlMo_2O_8$ heat-treated at different temperatures was also performed. The corresponding X-ray diffraction patterns are presented in Fig. 3, respectively. The phase composition and estimation of crystallite sizes for obtained ceramics were determined by the Rietveld refinement. The homogeneity of the as-synthesised gel precursor was proven by the lower diffractogram of

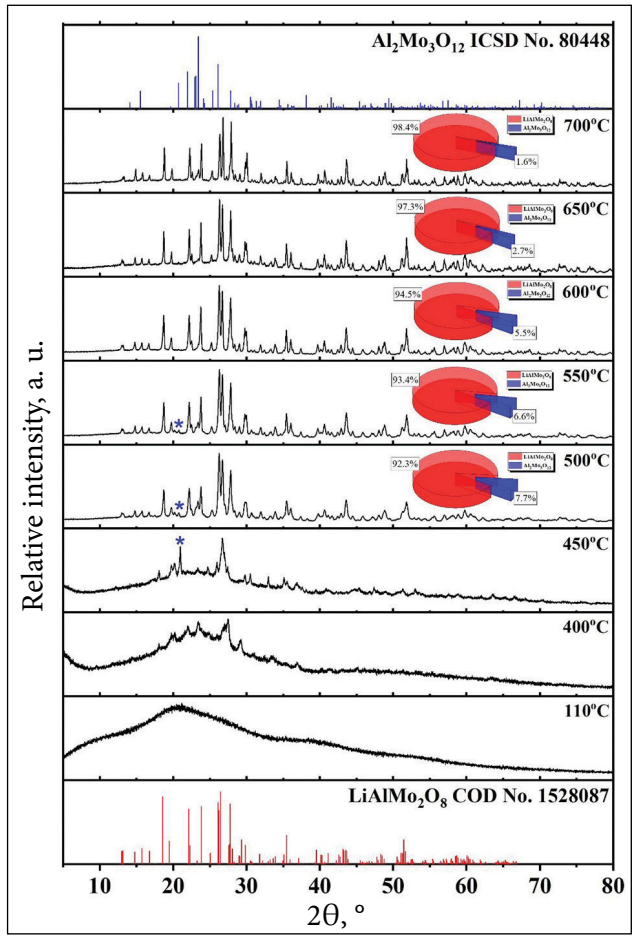

Fig. 3. Standard COD and ICSD cards for the $LiAlMo_2O_8$ and $Al_2Mo_3O_{12}$ crystalline phases and powder XRD patterns for the Li–Al–Mo–O tartrate gel precursor sample dried at 110°C and heat-treated at different temperatures

Fig. 3, in which no characteristic peaks attributable to crystalline compounds were observed. As shown in the results of the thermal analysis, after the decomposition processes of the excess tartaric acid, the beginning of the crystallisation of crystalline compounds is distinguished. Knowing that the formation of aluminium molybdate starts above the temperature of 400°C, heat treatment of the sample at 450°C leads to the formation of at least two different crystalline phases. Nevertheless, the composition of the remaining crystalline phases of the Li–Al–Mo–O gel precursor heat-treated at higher temperatures shows the dominance of the triclinic $LiAlMo_2O_8$ compound whose amount tends to increase by increasing the heat-treatment temperature. Meanwhile, the crystallite growth trends of the $LaAlMo_2O_8$ ceramic are shown in Fig. 4. In this case, the size of crystallites increases exponentially from 36.75 nm for the sample heat-treated at 500°C to 126.11 nm at 700°C. It should also be noted that the existence of the impurity $Al_2Mo_3O_{12}$ crystalline phase coincides with the conclusions obtained by analysing the results of the thermal analysis when the observed decrease in the mass of the sample above the temperature of 900°C was associated with the decomposition of aluminium molybdate and the removal of MoO_3 from the reaction mixture.

Summarising the results obtained from XRD diffractograms, it can be concluded that the composition of the final crystalline phases in the reaction mixture significantly depends on the molar composition of the initial reagents. Thus, the increase in the heat-treatment temperature reduces the number of impurity phases in the reaction mixture; however, the synthesis of single-phase $LiAlMo_2O_8$ compound at lower temperature remains complicated.

SEM micrographs

In order to show the tendency of particle growth of the obtained ceramics by increasing the heat-treatment temperature, the surface morphology was investigated. Corresponding SEM micrographs of the Li–Al–Mo–O tartrate gel precursor heat-treated at 400, 500, 600 and 700°C are shown in Fig. 5. In the SEM picture of part (a) for Fig. 5, the surface of the sample is homogeneous, consisting of irregularly shaped formations formed during the decomposition of unreacted tartaric acid. This result is in good agreement with the XRD data when the formation of the final ceramic at 400°C temperature is not clearly expressed. As seen from the Fig. 5 micrograph (b), the increase of the heat-treatment temperature of the sample up to 500°C shows the changes in the surface morphology associated with the start of the growth of spherical

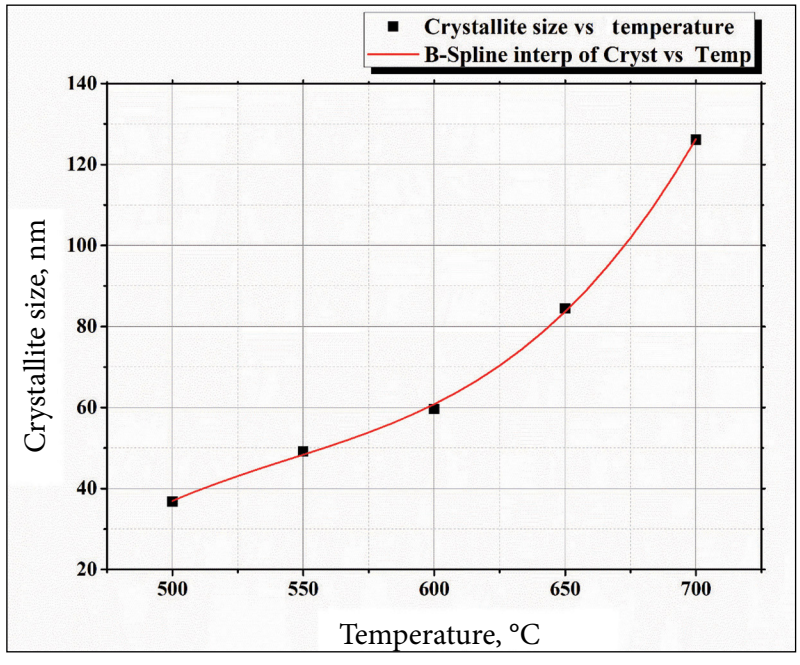

Fig. 4. Growth trends of the crystallites for $LiAlMo_2O_8$ ceramic

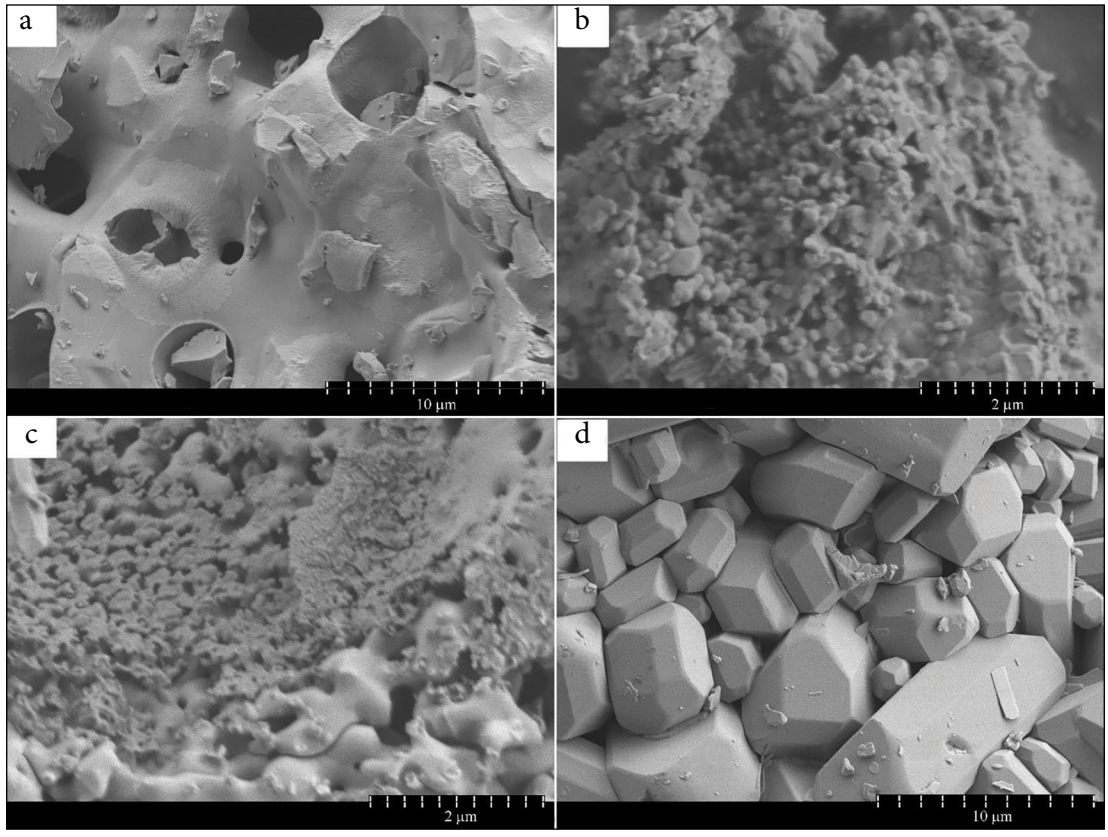

Fig. 5. SEM micrographs of the Li–Al–Mo–O tartrate gel precursor for the $LiAlMo_2O_8$ ceramic heat-treated at the temperatures of 400°C (a), 500°C (b), 600°C and 700°C (d) in the air atmosphere

particles with a size smaller than 200 nm. An almost identical view is observed for the gel precursor heat-treated at 600°C temperature, in which a well-seen agglomeration of smaller particles into large aggregates is distinguished. Finally, the heat-treatment of the sample at 700°C forms the particles of a regular shape with well-defined edges, ranging in a size from 4 to 10 µm.

Thus, the SEM results indicate that the growth of the particles of the final ceramic takes place in two stages. In the first step, the formation of the agglomerates of crystallites whose diameter does not exceed 100 nm is distinguished. Meanwhile, above 400°C temperature, the formed particles start to combine into formations of 4–10 µm in size with a regular structure, clear planes and well-expressed edges. Based on the results of XRD analysis, it can be concluded that the regularly shaped particles are mainly composed of crystallites, the average size of which corresponds to the value of 126.11 nm.

FT-IR analysis

By continuing, further studies on the Li–Al–Mo–O tartrate gel precursor heat-treated at different temperatures infrared spectroscopy (IR) was performed (Fig. 6) as an important investigation technique, which enables the fixation of the vibrational frequency of bonds for the crystalline ceramic with the initial composition of $LiAlMo_2O_8$. Generally, the infrared bands for inorganic materials are broader, fewer in number and appear at lower wavenumbers than those observed for organic materials [19]. Nevertheless, in the FT-IR spectrum of the sample heat-treated at 400°C, a broad band with weakly expressed peaks in the range from 1600 to 1050 cm^{-1} is attributable to the characteristic vibrations for chemical bonds of corresponding tartrates. In this case, the peak at 1589 cm^{-1} corresponds to the asymmetric stretching of the –COO functional group. Meanwhile, the peak position at 1380 cm^{-1} describes either –OH in-plane bending or –COO symmetric stretching. In summary, the –COO asymmetric and symmetric stretching vibrations combined with –OH in-plane bending vibrations are observed at ~1589 and ~1380 cm^{-1}, respectively [20]. The peaks that correspond to the values of 1256, 1121 and 1074 cm^{-1} are attributed to the C–H in-plane stretching [21], C–OH and

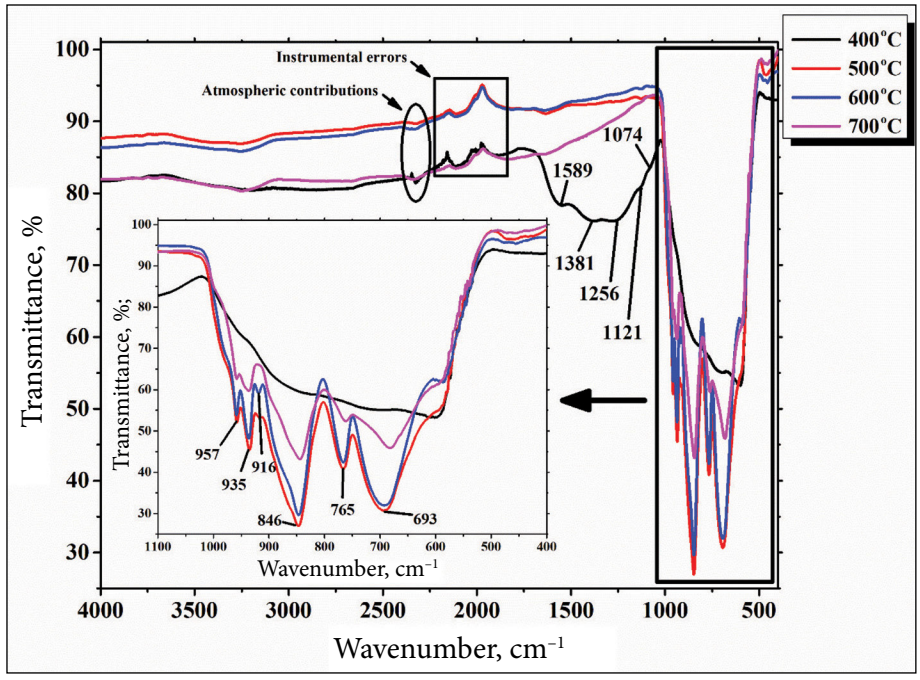

Fig. 6. FT–IR transmittance spectra of the Li–Al–Mo–O tartrate gel precursors for $LiAlMo_2O_8$ ceramic heat-treated at 400, 500, 600 and (d) 700°C of temperature

CH–OH stretching [22]. The relatively low intensity of the characteristic peaks attributable to the organic compounds can be explained by the complete decomposition of tartaric acid and the evaporation of the as-formed volatile components, and the existence of partially decomposed metal tartrates.

By increasing the heat-treatment temperature, the peaks of organic compounds in the range from 1600 to 1050 cm^{-1} tend to disappear. Meanwhile, the newly formed characteristic peaks, identified in the wavenumber range from 1000 to 500 cm^{-1}, correspond to the vibrations of the metal–oxygen bond. In this case, the peaks attributable to the ~957 and ~935 cm^{-1} wavenumber correspond to the characteristic vibrations of the symmetric MoO_4 tetrahedron. Meanwhile, a triply degenerate mode (ν_3) of F_2 symmetry for $\nu_{as}(MoO_4)$ and $\nu(Mo_2O_2)$ bridge vibrations correspond to the peaks at ~916, ~846, ~765 and ~693 cm^{-1}, respectively [23–25].

The intensity, width and shape of the peaks in the range from 1000 to 500 cm^{-1} depend on several factors such as the degree of crystallinity, surface area and crystal structure of the ceramic precursor. By increasing the heat-treating temperature, the crystallinity of crystalline compounds also increases. Meanwhile, the opposite effect is observed when the crystallites and particles tend to grow and the surface area has a tendency to decrease [26]. This is the main reason that determines the decrease in the intensity of the characteristic peaks of the gel precursor heat-treated at 700°C.

CONCLUSIONS

The thermal analysis of the Li–Al–Mo–O tartrate gel precursor for the $LiAlMo_2O_8$ ceramic allowed the estimation of the decomposition process and enabled the determination of the formation of impurity phases, especially the existence of lithium oxide in the ceramic mixture. By combining TGA/DTA and XRD characterisation techniques, the reasons for the change in the amount of the impurity $Al_2Mo_3O_{12}$ compound and its concentration decrease in the final $LiAlMo_2O_8$ multicomponent oxide were determined. The exponential trend in the temperature effect of crystallite growth for the $LiAlMo_2O_8$ ceramic from the XRD patterns was calculated by the X'Pert HighScore Plus software. The identical behaviour of the particle growth on the heat-treatment for the corresponding ceramic was confirmed by the SEM analysis. Finally, the FT-IR spectroscopy confirmed the high homogeneity of the synthesised Li–Al–Mo–O tartrate gel precursor. Moreover, it was shown that the degree of crystallinity and surface morphology significantly affects the intensity of characteristic bands.

ACKNOWLEDGEMENTS

This article is dedicated to the anniversary of Prof. Rimantas Ramanauskas.

Received 11 October 2022
Accepted 18 October 2022

References

1. L. Feng, L. Li, M. Zhang, Y. Yang, X. Sun, *Ceram. Int.*, **48**, 30630 (2022).
2. A. Sarapulova, D. Mikhailova, A. Senyshyn, H. Ehrenberg, *J. Solid State Chem.*, **182**, 3262 (2009).
3. L. Li, J. Zhang, W. Zi, S. Gan, G. Ji, H. Zou, X. Xu, *Solid State Sci.*, **29**, 58 (2014).
4. V. Volkov, C. Cascales, A. Kling, C. Zaldo, *Chem. Mater.*, **17**, 291 (2005).
5. Y. Xiao, L. Feng, B. Huang, J. Chen, W. Xie, X. Sun, *Ceram. Int.*, **47**, 29856 (2021).
6. X. Feng, L. Wang, R. Wei, Z. Wang, *J. Am. Ceram. Soc.*, **103**, 1046 (2020).
7. M. Gancheva, T. Rojac, R. Iordanova, I. Piroeva, P. Ivanov, *Ceram. Int.*, **48**, 17149 (2022).
8. S. Raghunath, R. Balan, *Mater. Today: Proc.*, **46**, 2930 (2021).
9. A. Phuruangrat, S. Thongtem, T. Thongtem, *Mater. Res. Innov.*, **26**, 84 (2022).
10. P. Nayak, S. S. Nanda, S. K. Gupta, K. Sudarshan, S. Dash, *J. Am. Ceram. Soc.* (2022).
11. Y. Huang, X. Liu, Y. Jiang, X. Zhu, *Ceram. Int.*, **47**, 11654 (2021).
12. T. Li, C. Guo, Y. Wu, L. Li, J. H. Jeong, *J. Alloys Compd.*, **540**, 107 (2012).
13. T. Li, C. Guo, P. Zhao, L. Li, J. H. Jeong, *J. Am. Ceram. Soc.*, **96**, 1193 (2013).
14. J. Kim, *Inorg. Chem.*, **56**, 8078 (2017).
15. A. Das, H. P. Dasari, M. Saidutta, *Ceram. Int.*, **48**, 29229 (2022).
16. J. J. Cruywagen, J. B. B. Heyns, E. A. Rohwer, *J. Chem. Soc. Dalton*, **6**, 1951 (1990).
17. A. Žalga, G. Gaidamavičienė, Ž. Gricius, et al., *J. Therm. Anal. Calorim.*, **132**, 1499 (2018).
18. M. L. Ruiz, I. D. Lick, M. I. Ponzi, et al., *Thermochim. Acta*, **499**, 21 (2010).
19. L. Cavalcante, J. Sczancoski, J. Espinosa, J. A. Varela, P. Pizani, E. Longo, *J. Alloys Compd.*, **474**, 195 (2009).
20. B. Fu, Q. Shen, W. Qian, Y. Zeng, X. Sun, M. Hannig, *J. Mater. Sci. Mater. Med.*, **16**, 827 (2005).
21. V. Sasikala, D. Sajan, N. Vijayan, K. Chaitanya, M. B. Raj, B. S. Joy, *Spectrochim. Acta A Mol. Biomol. Spectrosc.*, **123**, 127 (2014).
22. Z. Dega-Szafran, G. Dutkiewicz, Z. Kosturkiewicz, M. Szafran, *J. Mol. Struct.*, **889**, 286 (2008).
23. M. Mączka, J. Hanuza, A. Pietraszko, *J. Solid State Chem.*, **154**, 498 (2000).
24. J. Hanuza, M. Maczka, *Vib. Spectrosc.*, **7**, 85 (1994).
25. V. M. Pillai, T. Pradeep, M. Bushiri, R. Jayasree, V. Nayar, *Spectrochim. Acta A Mol. Biomol. Spectrosc.*, **53**, 867 (1997).
26. G. Gaidamavičienė, A. Žalga, *Mater. Chem. Phys.* **241**, 122339 (2020).

Artūras Žalga, Austėja Diktanaitė, Giedrė Gaidamavičienė

LIČIO ALIUMINIO MOLIBDATO ($LiAlMo_2O_8$) SINTEZĖ VANDENINIU ZOLIŲ-GELIŲ METODU, TERMINĖ, STRUKTŪRINĖ IR SPEKTROSKOPINĖ ANALIZĖ

Santrauka

Šiame darbe vandeninis zolių-gelių sintezės metodas buvo sėkmingai pritaikytas homogeniško tartratinio Li–Al–Mo–O gelio sintezei. Termogravimetrinė ir diferencinė skenuojančioji kalorimetrinė analizė leido paaiškinti gautojo gelio pirmtako terminio skilimo eigos mechanizmą ir įvertinti priemaišinių fazių $LiAlMo_2O_8$ trikomponenčiame okside susidarymo priežastis bei mažėjimo tendencijas. O rentgeno spindulių difrakcinė analizė aiškiai parodė ne tik 400, 450, 500, 550, 600, 650 ir 700 °C temperatūrose iškaitintų pavyzdžių kristalinę sudėtį, tačiau, atlikus matematinius skaičiavimus, patvirtino eksponentinę $LiAlMo_2O_8$ fazės kristalitų augimo eigą. Pasitelkus skenuojančiąją elektroninę mikroskopiją patvirtintas dalelių augimas, didinant kaitinimo temperatūrą. Galiausiai, infraraudonųjų spindulių spektroskopija padėjo susieti besiformuojančių galutinio kristalinio junginio dalelių paviršiaus ploto mažėjimą su charakteringųjų Mo–O cheminių ryšių vibracijų intensyvumais.